Turk J Elec Engin, VOL.13, NO.1 2005, © TÜBİTAK

Transformer Protection Using the Wavelet Transform

Okan ÖZGÖNENEL, Güven ÖNBİLGİN, Çağrı KOCAMAN
Ondokuz Mayis University, Electrical & Electronics Engineering Faculty,
55139, Kurupelit, Samsun-TURKEY
e-mail: okanoz@omu.edu.tr, gonbilgi@omu.edu.tr, ckocaman@omu.edu.tr

Abstract

This paper introduces a novel approach for power transformer protection algorithm. Power system signals such as current and voltage have traditionally been analysed by the Fast Fourier Transform. This paper aims to prove that the Wavelet Transform is a reliable and computationally efficient tool for distinguishing between the inrush currents and fault currents. The simulated results presented clearly show that the proposed technique for power transformer protection facilitates the accurate discrimination between magnetizing inrush and fault currents in transformer protection.

Key Words: *Differential Protection, Power Transformer, Discrete Wavelet Transform (DWT), Fast Fourier Transform (FFT), Discontinuity Analysis.*

1. Introduction

Transformers are essential and important elements of power systems. Due to their sizes and varieties, protection approaches of power transformers differ depending on the situation. For small distribution transformers of less then 1.5 MVA, high rupturing capacity (HRC) fuse will suffice. Others use overcurrent relays. However, for the larger power transformers, differential protection based on circulating current principle is usually adopted. The differential protection converts the primary and secondary currents to a common base and compares them. The difference between these currents is small during normal operating conditions. The difference is also small for external faults, but is larger than the difference for normal operating conditions. However, during an internal fault in a transformer, the difference becomes significant. The differential protection is then based on matching the primary and secondary current of the transformer for ideal operation. When a transformer is switched off, its core generally retains some residual flux. Later, when the transformer is re-energized, the core is likely to saturate. If the transformer is saturated, the primary windings draw large magnetizing currents from the power system. These results in a large differential current which cause the differential protection relay to operate.

Due to the numerous benefits of digital relaying in terms of economics, performance, reliability and flexibility, significant efforts have been made towards the development of digital relaying algorithms. Numerous algorithms for the differential protection of power transformers have been proposed [1], [2], [3]. Generally, an acceptable protection scheme involves features: reliability, cost, simplicity to use and high speed of operation.

Traditional digital protective relays present several drawbacks; for instance, they are usually based on algorithms that estimate the fundamental component of the current and voltage signals neglecting higher frequency transient components. Moreover, phasor estimation requires a sliding-window of a cycle that may cause a significant delay. Furthermore, accuracy is not assured. The Fourier transform is a very useful tool for analyzing the frequency content of stationary processes. When dealing with non-stationary processes, however, other methods for determining the frequency content must be applied [4].

For this reason wavelet decomposition is ideal for studying transient signals and obtaining a much better current characterization and a more reliable discrimination. Wavelets allow the decomposition of a signal into different levels of resolution (frequency octaves). The basis function (Mother Wavelet) is dilated at low frequencies and compressed at high frequencies, so that large windows are used to obtain the low frequency components of the signal, while small windows reflect discontinuities [5].

Wavelet transform has a special feature of variable time – frequency localization which is very different from windowed Fourier transform. In a recent study, wavelet transform has been used on an experimental three phase transformer to analyze the instantaneous magnetizing current and to identify fault conditions with the choice of Daubechies 4 type wavelets [6]. Hence, wavelet decomposition of the first level has been employed with the consequence of limited details and sensivity. As well as employing a Coiflet 6 family of wavelets to provide sufficient details and sensivity.

The main objective of this paper is to analyse discontinuities in current signals during phase to ground faults and phase to phase faults.

2. Wavelets

Differential protection algorithms based on FFT have disadvantages including the neglecting of high frequency harmonics. Furthermore, different windowing techniques should be applied to calculate the current and voltage phasors and this causes significant time delay for the protection relay. In this case, accuracy is not assured completely. Due to increased standards of the delivered energy quality such as IEEE 519, high performance algorithms should be taken into account.

The Grossmann & Morlet (1984) definition of the continuous wavelet transform (CWT) for a 1-D signal $f(x) \in L^2(R)$ is

$$\begin{aligned} W(a,b) &= k(a) \int_{-\infty}^{\infty} f(x) \bar{\psi}\left(\tfrac{b-x}{a}\right) dx \\ &= k(a) \int_{-\infty}^{\infty} f(x) \widetilde{\psi}\left(\tfrac{x-b}{a}\right) dx \end{aligned} \tag{1}$$

where $\widetilde{\psi}(x) = \bar{\psi}(x)$; $a \in R^+$ and $b \in R$, are the scale and the position parameters, respectively, with R^+ being the set of positive real numbers; $L^2(R)$ denotes the Hilbert space of square integrable functions, and the bar denotes the conjugated complex. The constant $k(a)$ can be taken to be $1/\sqrt{a}$ in order to insure normalization in energy of the set of wavelets $\psi\left(\frac{x-b}{a}\right)$ obtained by a translation and dilation of the "mother wavelet" ψ. The first formula permits the interpretation of the wavelet transform as a convolution product; the second as a correlation function. If the wavelet is symmetric and real $\widetilde{\psi} = \bar{\psi}$(as in the case of the Poission wavelet) both notions coincide (Moreau *et al.* 1997).

The main advantage of the CWT is that it reveals the signal content in far greater detail than either Fourier analysis or the discrete wavelet transform (DWT). The continuous nature of the wavelet function is kept up to the point of sampling the scale-translation grid used to represent the wavelet transform is independent of the sampling of the signal under analysis.

In this case, the discrete wavelet transform is

$$\widetilde{W}_{l,k} = \int_{-\infty}^{\infty} f(x)\psi_{l,k}(x)dx \tag{2}$$

and the inverse discrete transform (IDWT) is

$$f(x) = \sum_{l=-\infty}^{\infty} \sum_{k=-\infty}^{\infty} \widetilde{W}_{l,k}\psi_{l,k}(x) \tag{3}$$

in the L^2- sense.

The advantage of analysing a signal with wavelets is that it enables one to study the local features of the signal with a detail matched to their characteristic scale. In the temporal domain such a property allows for an effective representation of transient signals. We can say that the DWT enables one to make a *multiresolution analysis* of a signal. It is possible to have both smooth wavelets with compact support and symmetry of the associated scaling functions and this avoids bias for the locations of maxima and minima of the signal [7].

The Wavelet Transform is well suited to the problem in this study. It is similar to the Fourier transform, but uses a basis function that decays rapidly from a central feature rather than the infinite sine function. For this reason wavelet decomposition is ideal for studying transient signals and obtaining a much better current characterization and a more reliable discrimination.

The application areas of wavelets cover time and frequency analysis, electromagnetic analysis, filters, integral equations, transient analysis, picture processing, and data compressing techniques.

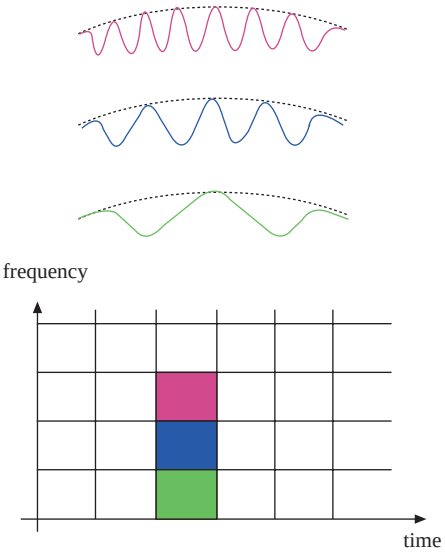

Figure 1. Gabor localizes the short time fast Fourier Transform (STFFT) in 1945.

In Figure 1, time and frequency localization are shown for the short time fast Fourier Transform. This approach was presented by Gabor in 1945.

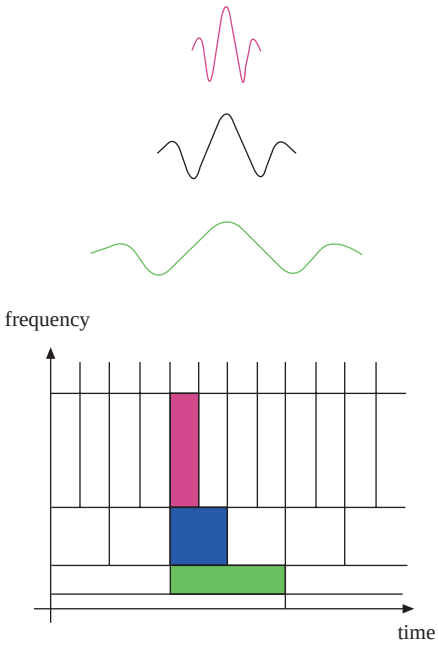

Figure 2. Morlet proposes the continuous wavelet transform in 1980.

In Figure 2, time and frequency localization are shown for the continuous wavelet transform. This approach was presented by Morlet in 1980.

2.1. Selection of Wavelet Functions

Wavelet transforms are fast and efficient means of analyzing transient voltage and current signals. In this work, Coiflet 6 (Coif 6) wavelet function has been used for the discontinuity analysis of phase currents. Different kinds of wavelets families are derived. Coif 6 is simply chosen since it gives a more accurate solution and minimum reconstruction error during the magnetizing inrush condition and fault conditions.

Coiflet wavelets are designed for the purpose of maintaining a close match between the trend values and the original signal values. Following a suggestion of Coifman, these wavelets first constructed by Daubechies, who called them "coiflets". All of the coiflet wavelets are defined in a similar way; so this paper shall concentrate on the simplest case of Coif 6 wavelets [8], [9]. The scaling numbers for the Coif 6 scaling signals are listed below:

The following equations describe steps of deriving Coif6 wavelet and scale functions used in this paper step by step.

$$\alpha_1 = \frac{1-\sqrt{7}}{16\sqrt{2}}, \quad \alpha_2 = \frac{5+\sqrt{7}}{16\sqrt{2}}, \alpha_3 = \frac{14+2\sqrt{7}}{16\sqrt{2}}, \alpha_4 = \frac{14-2\sqrt{7}}{16\sqrt{2}}, \alpha_5 = \frac{1-\sqrt{7}}{16\sqrt{2}}, \alpha_6 = \frac{-3+\sqrt{7}}{16\sqrt{2}}$$

Using these scaling numbers, the first level Coif6 scaling signals defined by

$$\begin{aligned}
V_1^1 &= (\alpha_1, \alpha_2, \alpha_3, \alpha_4, \alpha_5, \alpha_6, 0, 0....) \\
V_2^1 &= (0, 0, \alpha_1, \alpha_2, \alpha_3, \alpha_4, \alpha_5, \alpha_6, 0, 0....) \\
V_3^1 &= (0, 0, 0, 0, \alpha_1, \alpha_2, \alpha_3, \alpha_4, \alpha_5, \alpha_6, 0, 0....) \\
&.. \\
&.. \\
V_{\frac{N}{2}-1}^1 &= (0, 0, 0, ...\alpha_1, \alpha_2, \alpha_3, \alpha_4, \alpha_5, \alpha_6, 0, 0) \\
V_{\frac{N}{2}}^1 &= (\alpha_3, \alpha_4, \alpha_5, \alpha_6, 0, ...0, 0, \alpha_1, \alpha_2, 0, 0)
\end{aligned} \tag{4}$$

where N is number of samples.

As a generalized expression, equation (4) can be re-written as follows.

$$V_m^1 = \alpha_1 V_{2m-1}^0 + \alpha_2 V_{2m}^0 + \alpha_3 V_{2m+1}^0 + \alpha_4 V_{2m+2}^0 + \alpha_5 V_{2m+3}^0 + \alpha_6 V_{2m+4}^0 \tag{5}$$

The Coif6 wavelet numbers are defined by $\beta 1 = \alpha 6$, $\beta 2 = -\alpha 5$, $\beta 3 = \alpha 4$, $\beta 4 = -\alpha 3$, $\beta 5 = \alpha 2$, $\beta 6 = -\alpha 1$ and these wavelet numbers determine the first – level Coif6 wavelets as follows:

$$\begin{aligned}
W_1^1 &= (\beta_1, \beta_2, \beta_3, \beta_4, \beta_5, \beta_6, 0, 0....) \\
W_2^1 &= (0, 0, \beta_1, \beta_2, \beta_3, \beta_4, \beta_5, \beta_6, 0, 0....) \\
W_3^1 &= (0, 0, 0, 0, \beta_1, \beta_2, \beta_3, \beta_4, \beta_5, \beta_6, 0, ...) \\
&.. \\
&.. \\
W_{\frac{N}{2}-1}^1 &= (0, 0, 0, ...\beta_1, \beta_2, \beta_3, \beta_4, \beta_5, \beta_6, 0, 0) \\
W_{\frac{N}{2}}^1 &= (\beta_3, \beta_4, \beta_5, \beta_6, 0, ...0, 0, \beta_1, \beta_2)
\end{aligned} \tag{6}$$

As a generalized expression, (6) can be re-written as:

$$W_m^1 = \beta_1 V_{2m-1}^0 + \beta_2 V_{2m}^0 + \beta_3 V_{2m+1}^0 + \beta_4 V_{2m+2}^0 + \beta_5 V_{2m+3}^0 + \beta_6 V_{2m+4}^0 \tag{7}$$

Inverse wavelet transform for Coif6 is expressed as:

$$F = A^1 + D^1 \tag{8}$$

In (8), A is called the *approximation* and D is called the *detail* signal where F is the synthesized signal. At level 1, A is defined as

$$A^1 = (F.V_1^1)V_1^1 + (F.V_2^1)V_2^1 + ... + (F.V_{N/2}^1)V_{N/2}^1 \tag{9}$$

At level 1, D is defined as

$$D^1 = (F.W_1^1)W_1^1 + (F.W_2^1)W_2^1 + ... + (F.W_{N/2}^1)W_{N/2}^1 \tag{10}$$

Inverse wavelet transform for Coif 6 at level 2 is expressed as

$$F = A^2 + D^2 + D^1 \tag{11}$$

At level 2, A is defined as:

$$A^2 = (F.V_1^2)V_1^2 + ... + (F.V_{N/4}^2)V_{N/4}^2 \tag{12}$$

At level 2, D is defined as:

$$D^2 = (F.W_1^2)W_1^2 + ... + (F.W_{N/4}^2)W_{N/4}^2 \tag{13}$$

Mallat's wavelet tree is chosen for the mathematical procedure summarized above

2.2. Proposed Protection Algorithm

The proposed protection algorithm is summarized as below step by step.

First Step: Acquiring the current and voltage signals obtained from transformer terminals and calculating orthogonal basis scale and mother wavelet vectors (V_N^m and W_N^m).

Second Step: The coefficient vectors, a^m and d^m, are calculated as below.

$$a^m = (discreet\_signal) * V_N^m,$$

$$d^m = (discreet\_signal) * W_N^m$$

Third Step: Approximation and Detail coefficients, A^m and D^m, are calculated as below:

$$A^m = a^m * V_N^m,$$

$$D^m = d^m * W_N^m$$

Fourth Step: Inverse wavelet transform

$$synthesized\_signal = A^m + D^m + ... + D^2 + D^1$$

A flowchart of the proposed algorithm is seen in Figure 3.

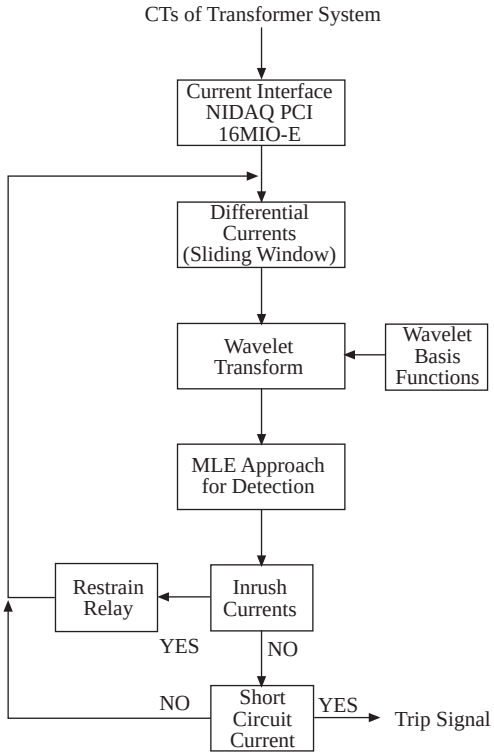

Figure 3. A flowchart of the proposed algorithm.

3. Simulation and Application

A system with a generator, a three phase transformer and a load has been simulated (Figure 4) using the ATP-EMTP software. Extensive series of simulation studies have been carried out to obtain fault transient signals for subsequence analysis.

Simulations include:

- 150 different types of energizing situations with different source triggering angles,
- 80 different types of faults on either the primary side or the secondary side of the transformer such as phase to phase and phase to ground faults with different source triggering angles.

To simulate high impedance fault identification, all faults are generated with a fault resistance.

The fundamental frequency is 50Hz and the sampling frequency is 2000Hz. This corresponds to 40 samples per cycle. 2000 Hz is chosen in order to capture the high frequency components of the signals and has been considered to be adequate for this case.

Similarly, phase to phase faults are also generated in both side of the transformer. A three phase – three windings laboratory transformer has been used and modeled in ATP-EMTP with the magnetization curve (given in Figure 5).

The proposed fault detection scheme is as follows: Input signals are preprocessed by a discrete wavelet transform (using Coif6) extracting information from the transient signals simultaneously in both time and frequency domains. After this procedure, approximation and detail coefficients of the fault current are obtained. Since approximation coefficients are the low frequency components, they are out of the scope of

this study. Variations of the detail coefficients are *distinctive* samples. Under normal conditions for steady state operation, variation of detail coefficients is a very low level one. If the detail coefficients have some spikes with respect to time, we can conclude that faults are developing or have developed.

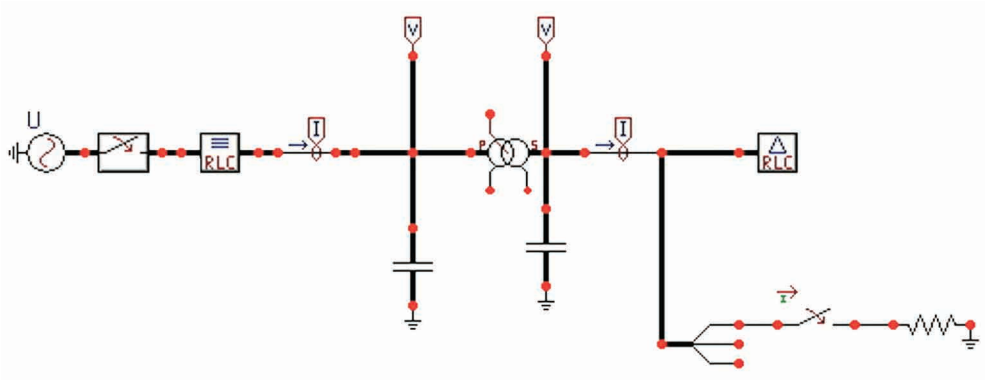

Figure 4. Simulated system. Phase to ground faults are generated at secondary side.

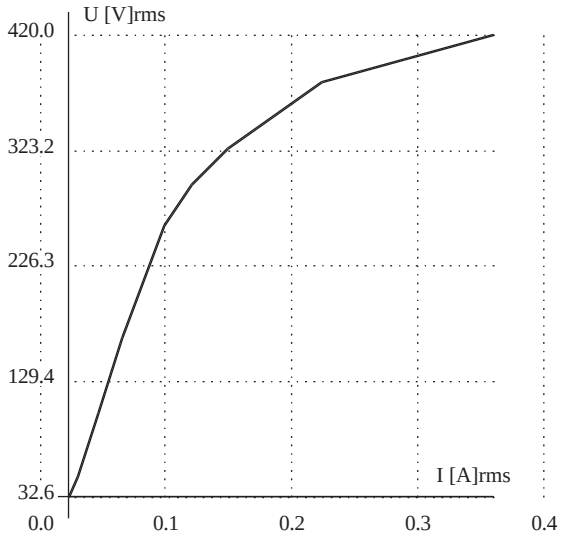

Figure 5. Magnetization curve of the transformer (220V/55V/55V, 50Hz, B=1Tesla, N_1=253 turns, N_2=53 turns, S=2100VA, S=30cm^2).

The next sections include ATP-EMTP simulations of a three phase – three windings laboratory transformers. These simulations include the case of magnetizing inrush, the case of single phase to ground fault, and the case of double phase to ground fault.

A. The Case of Magnetizing Inrush

In Figure 6, transformer is connected Yy0 and load resistances are chosen to be 1000Ω. Switching time is 5ms and phase angle of the supply is chosen $\delta = 0^o$ in order to simulate large magnetizing inrush current. In Figure 7, typical inrush current of the model transformer is seen with a connection of Yy0.

As it is seen from the Figure 7, duration of the magnetizing inrush for the laboratory transformer continues 200 ms. This time duration can easily be seen for the two phase currents after the decomposition of the inrush currents by using wavelets (see Figures 8 and 9).

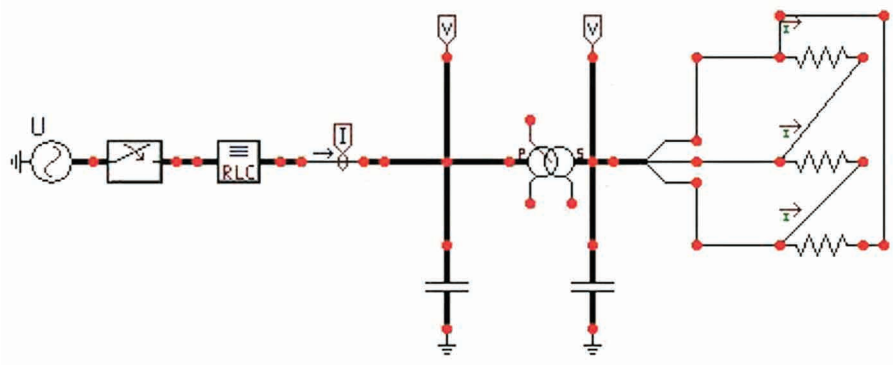

Figure 6. Simulation of magnetizing inrush current.

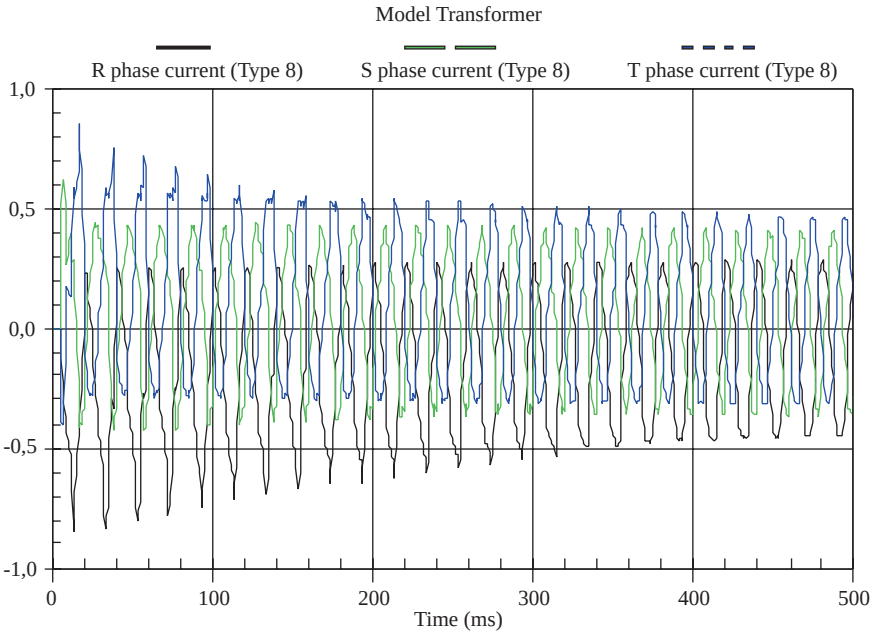

Figure 7. Typical inrush current of the model transformer.

As seen in Figure 8, variation of detail (D) coefficients is quite significant and shows the ability of detecting inrush currents. In this case, inrush currents are of large magnitudes until 0.3s and then tend to their normal operational levels. Similarly, Figure 9 shows magnetizing inrush currents and their wavelet decompositions.

B. The Case of Single Phase to Ground Fault

To obtain the simulation data, the test system seen in Figure 4 is used. The resistance at the fault location is chosen as 1Ω and transformer is assumed to have rated load $(5 + j6)\Omega$. The decomposition of the primary current and secondary voltage samples are seen in Figure 10a and (b). Fault time begins at 0.2s and cleared at 0.25s. Total fault time is 5ms.

As seen in Figures 10a and 10b, D coefficients give very distinctive solutions for fault current. The decomposition of the faulty phase currents have larger value of magnitude. This situation yields simplicity to interpret these coefficients. In a similar way, phase to phase fault currents can also be analysed.

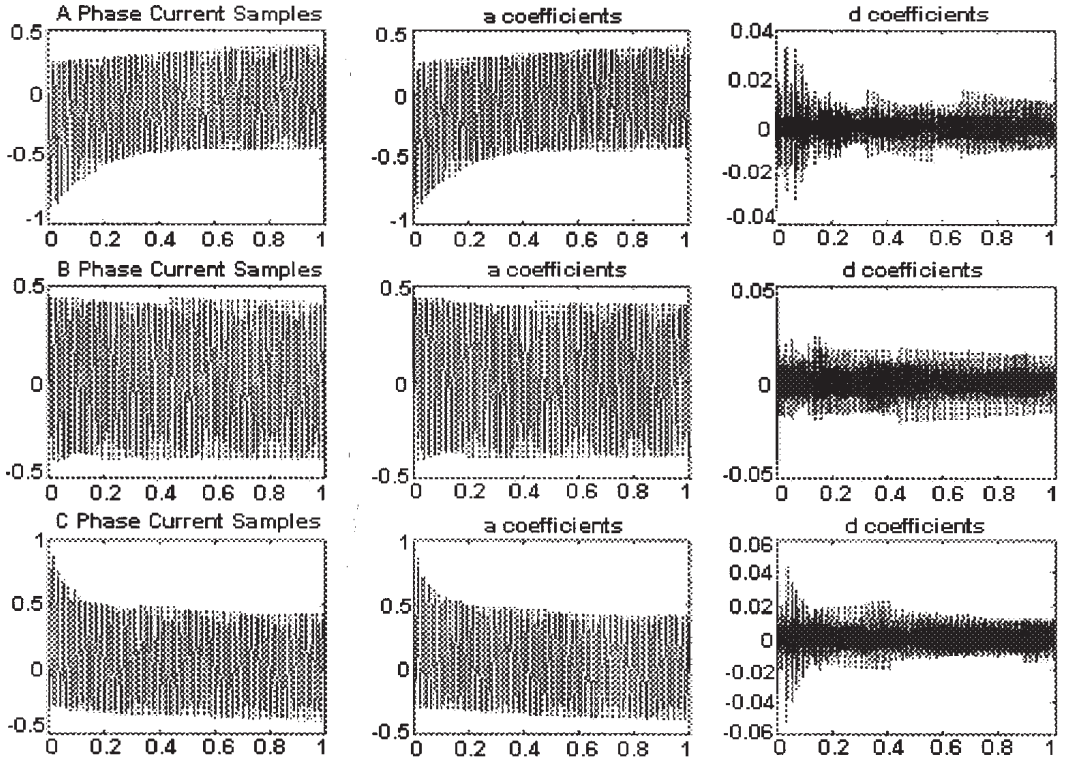

Figure 8. Decomposition of magnetizing inrush currents, $\delta = 0^o$.

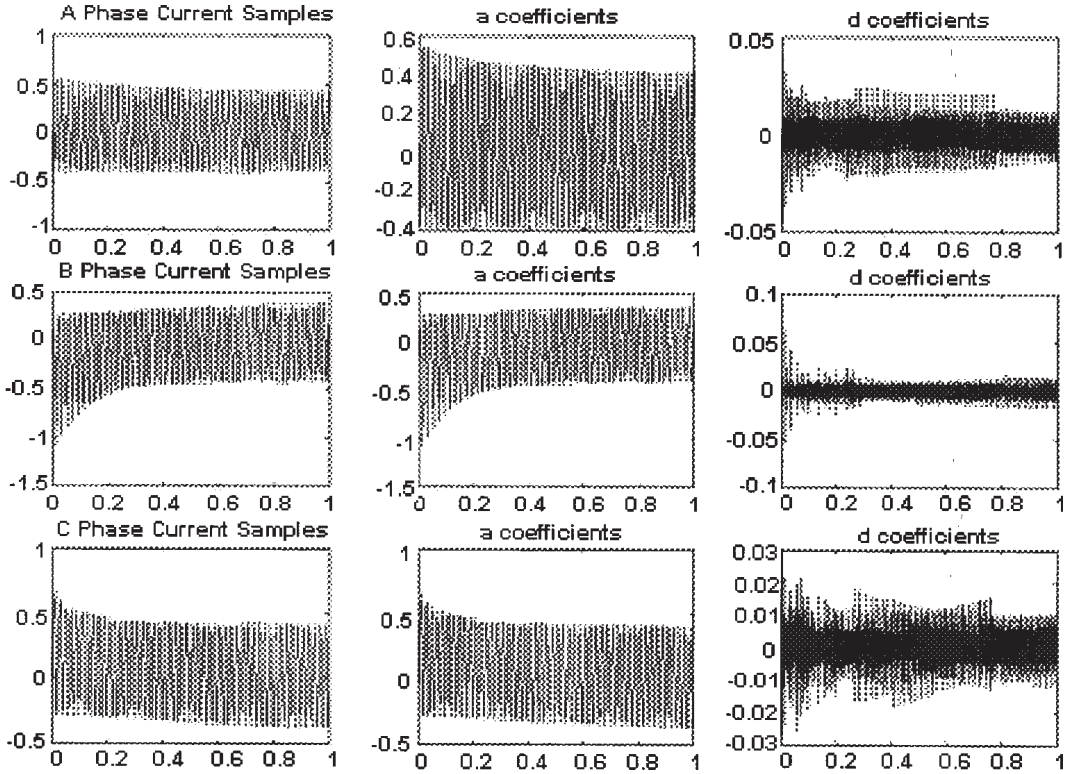

Figure 9. Magnetizing inrush currents in case of $\delta = 90^o$.

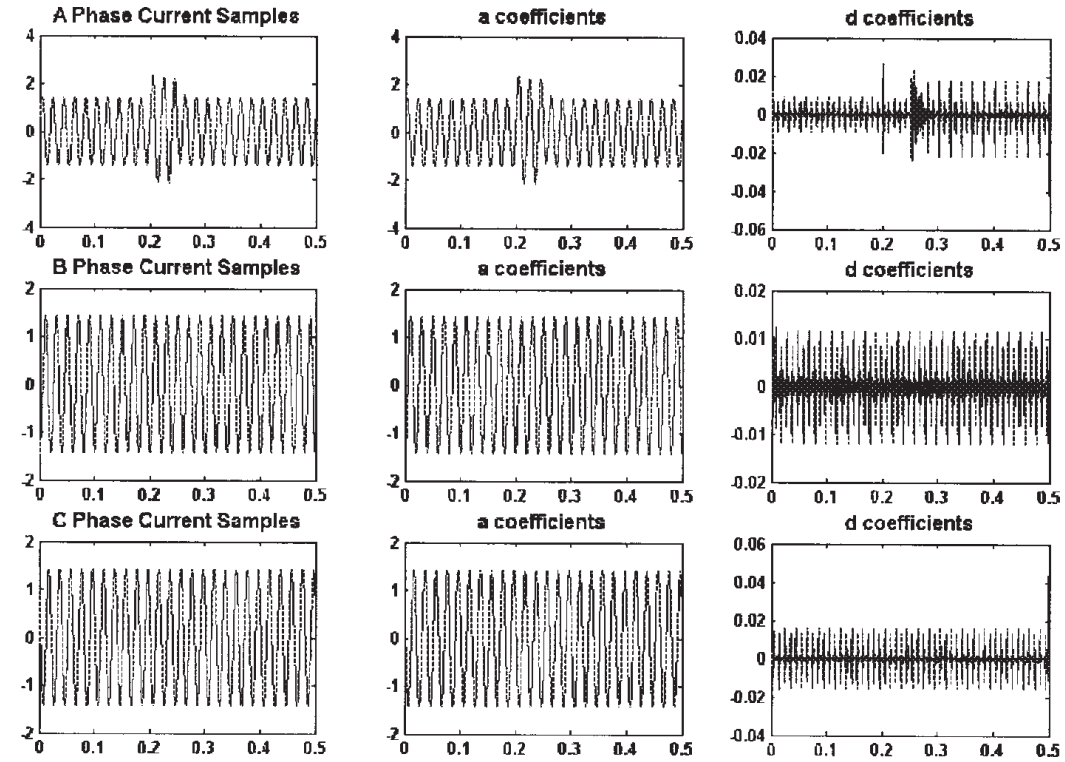

(a)

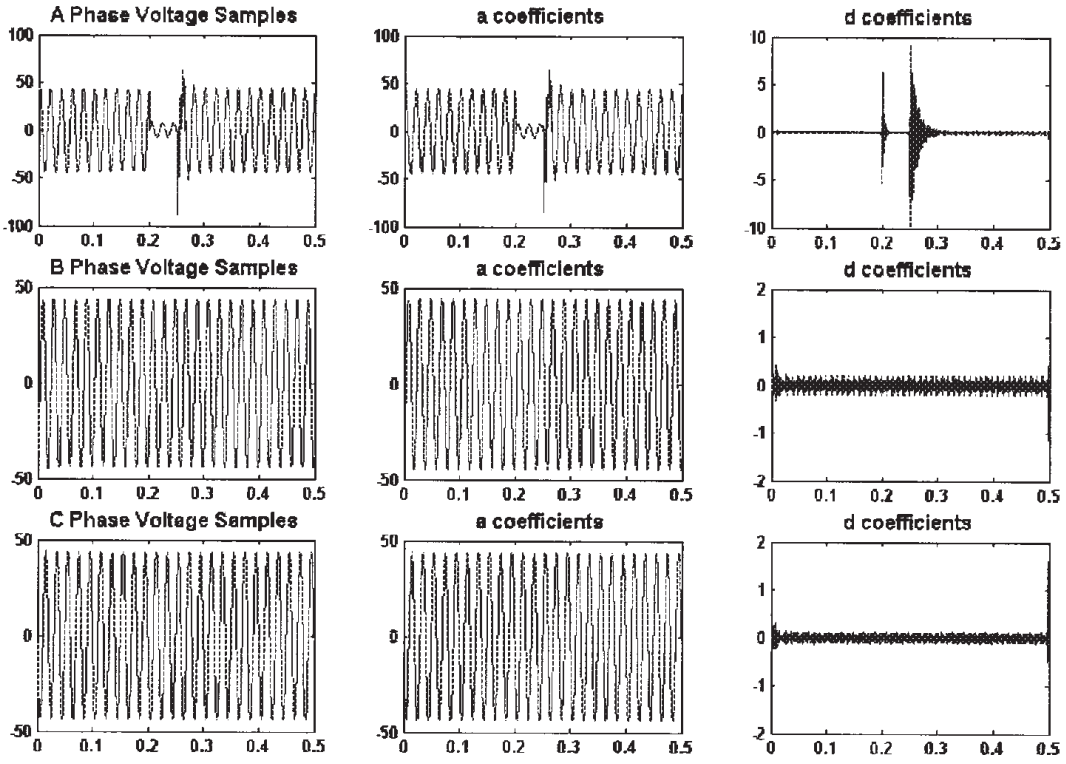

(b)

Figure 10. The case of single phase to ground fault. (a) Decomposition of primary currents, (b) Decomposition of

secondary voltages.

C. The Case of Double Phase to Ground Fault

To obtain the simulation data, the test system seen in Figure 11 is used. The resistance at the fault location (FR) is chosen as 1Ω and transformer is assumed to be on rated load $(5 + j6)\Omega$. Transformer is connected Dyn1. The decomposition of the primary current and secondary voltage samples are seen in Figures 12a and 12b. Fault commences at 0.2s and cleared at 0.25s. Total fault time is 5ms.

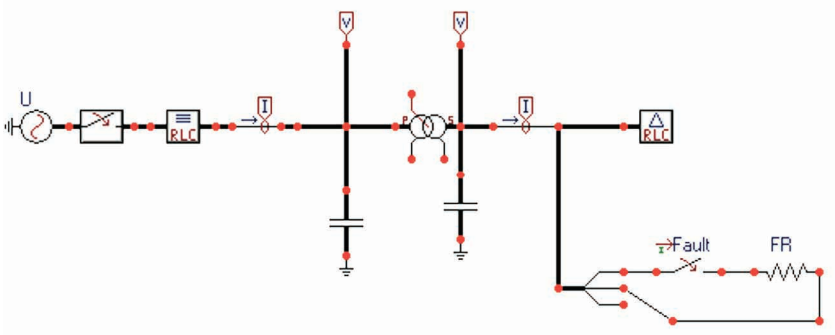

Figure 11. Simulation of phase – phase to ground fault.

In case of double phase to ground fault, the decomposition of the faulty phase currents have again larger value of magnitude and it is easily seen that A phase and B phase are interpreted as faulty phases in Figure 12. In Figures 10 and 12, horizontal axis is time while vertical one is magnitude.

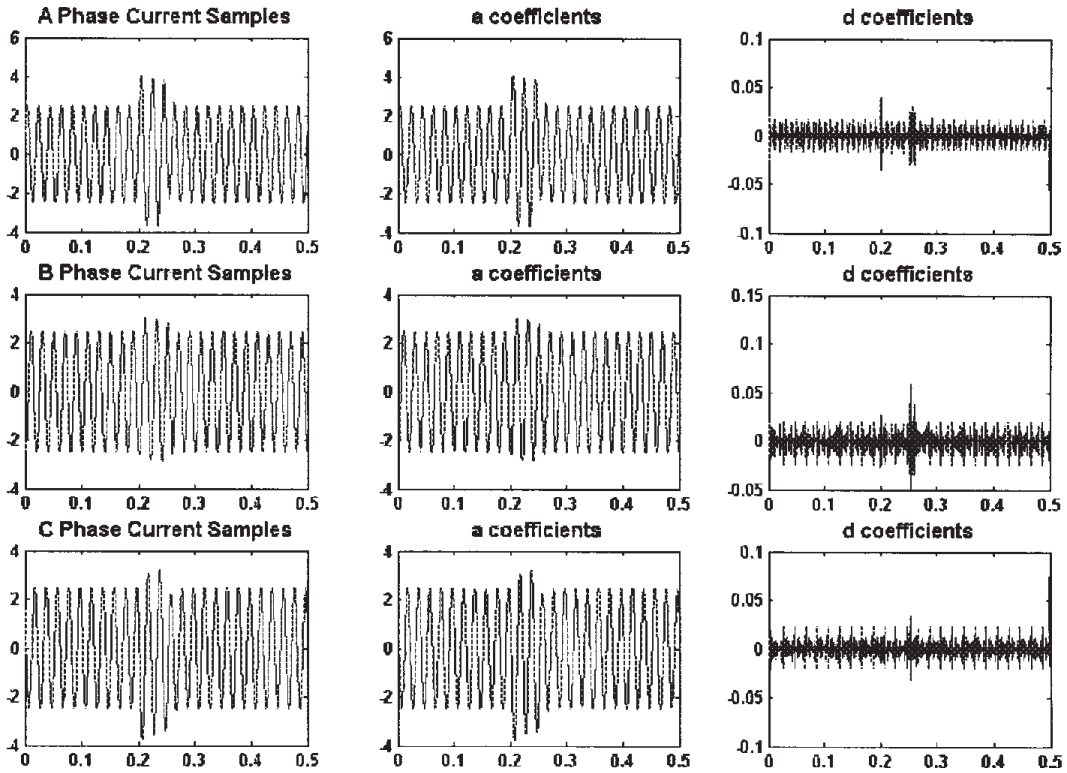

(a)

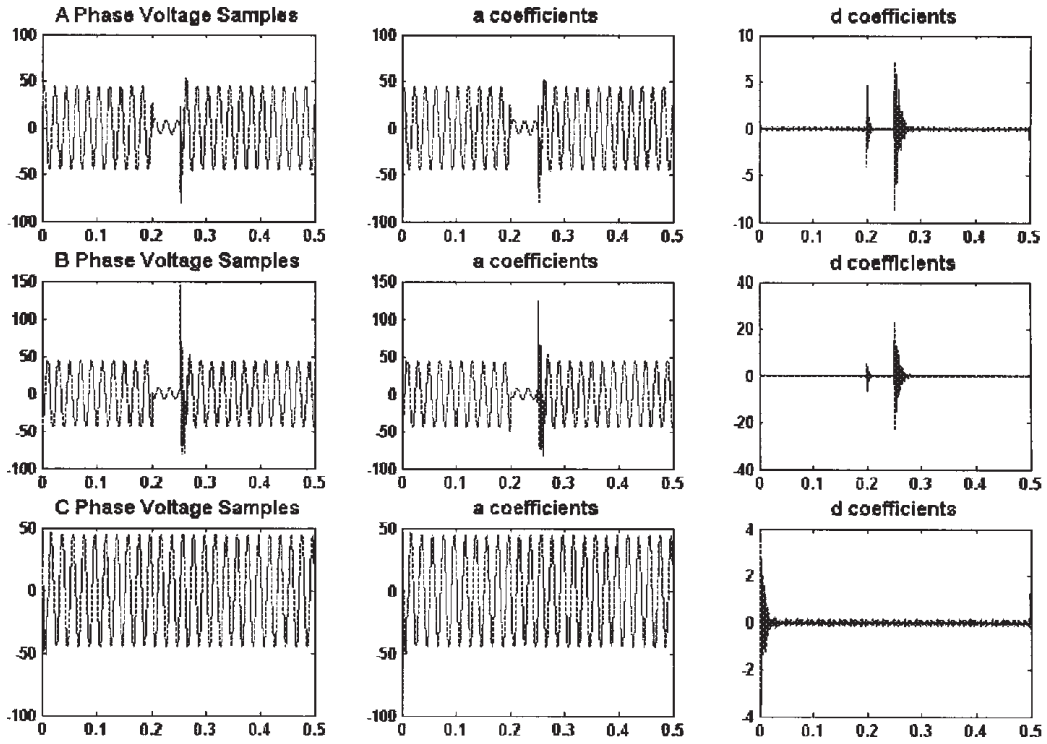

(b)

Figure 12. The case of two phases to ground fault. (a) Decomposition of primary currents, (b) Decomposition of secondary voltages.

As it is seen in Section 1, magnetizing inrush and fault currents are traditionally analyzed by using fast Fourier transform (FFT). In this case, if the ratio of second harmonic component to fundamental harmonic component exceeds a threshold value, wgich is generally taken about 20 %, the protection algorithm concludes an inrush condition and restrains relay not to send a trip signal. If the ratio of fifth harmonic component to fundamental harmonic component exceeds a threshold value, which is generally taken about 12 %, the protection algorithm concludes an outside fault condition and operates relay to send a trip signal.

Referring the Figures 8 and 9, which show magnetizing inrush condition with different source triggering angle, FFT of the inrush current is seen as Figure 13.

By using FFT, the ratio of second harmonic component to fundamental harmonic component is calculated 5.1 % and the ratio of fifth harmonic component to fundamental harmonic component is calculated 2.29 %. In this case, all samples of the inrush current (N) are taken into account. If N is chosen 500, the ratio of second harmonic component to fundamental harmonic component is calculated 10.57 % and the ratio of fifth harmonic component to fundamental harmonic component is calculated 4.32 %. If N is chosen 250, the ratio of second harmonic component to fundamental harmonic component is calculated 13.33 % and the ratio of fifth harmonic component to fundamental harmonic component is calculated 5.18 %. Since Fourier transform ideal for stationary signal, it is not well suited for non-stationary signals such as magnetizing inrush currents. Wavelet analysis is well suited for studying transient signals and obtaining a much better current characterization and a more reliable discrimination as summarized below.

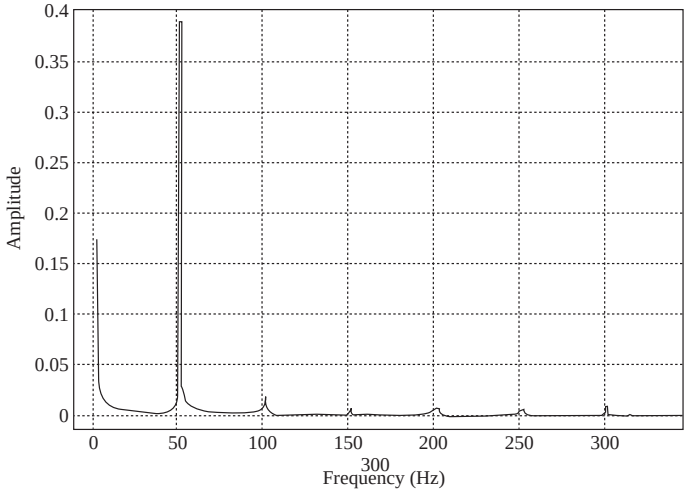

Figure 13. Fast Fourier transform of the inrush current.

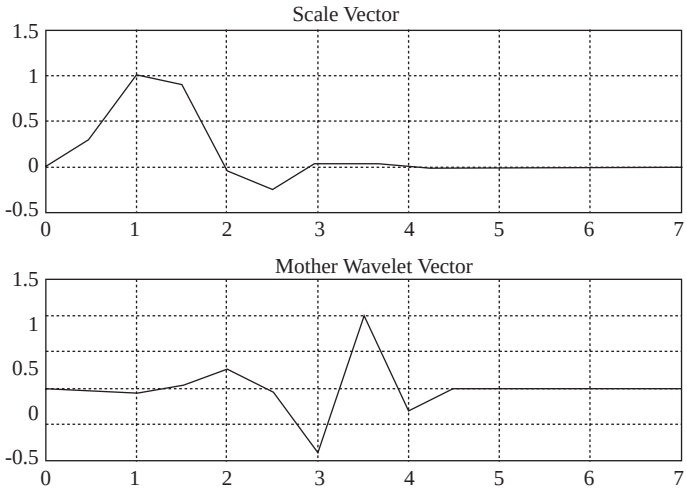

Figure 14. Daubechies 4 type scale and mother vectors at level 1.

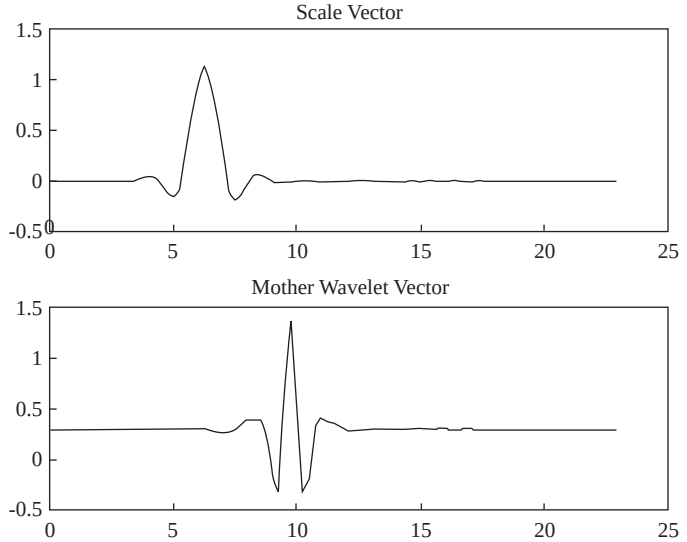

Figure 15. Coiflet 6 type scale and mother vectors at level 2.

Figure 14 and Figure 15 display the mother wavelets and scale vectors computed by Daubechies 4 and Coif6 wavelet respestively. It can be seen readily observed that Figure 15 shows clearly a marked improvement of Coif6 over the fast Fourier transform and Daubechies 4 wavelet transform.

4. Interpretation of Wavelet Coefficients

Recently, there are many ways of interpreting detail coefficients. In this work, maximum likelihood estimation is chosen for interpreting D coefficients. This method gives very sensitive estimations of fault current or voltage. Maximum likelihood estimation begins with a mathematical expression known as the Likelihood Function of the sampled data. Loosely speaking, the likelihood of a set of data is the probability of obtaining that particular set of data, given the chosen probability distribution model. This expression contains the unknown model parameters. The values of these parameters that maximize the sample likelihood are known as the maximum likelihood estimators or MLE's.

MLE is a totally analytic maximization procedure. It applies to every form of censored or multicensored data, and it is even possible to use the technique across several stress cells and estimate acceleration model parameters at the same time as life distribution parameters. Moreover, MLE's and likelihood functions generally have very desirable large sample properties [10], [11].

In this work, discrete uniform density function is used for interpreting D coefficients and results are quite adequate. For the laboratory transformer on rated load, the MLE values of currents and voltages (thresholds) change as below:

Threshold value of primary currents is about 0.2A and threshold value of secondary voltages is about 1.2V. These threshold values for primary currents and secondary voltages are MLE values of D coefficients.

A. Magnetizing Inrush Condition

Approximately, 150 different types of energizing situations, 20 rated load conditions, and 80 fault conditions have been simulated to assess the efficiency the proposed method.

During magnetizing inrush, for $\delta = 0^o$, the MLE values of D coefficients of each phase are calculated as

R phase = 0.0355
S phase = 0.0514
T phase = 0.0548

For $\delta = 0^o$, the value of D coefficient for a pure sine signal is calculated as 0.0056.

During magnetizing inrush, for$\delta = 90^o$, the MLE values of D coefficients of each phase are calculated as below:

R phase = 0.0480
S phase = 0.0637
T phase = 0.0349

Depending on the rated values of the transformer, these values can vary slightly. The proposed relay software blocks the relay to send a needless trip during inrush condition with the above D coefficients.

B. Phase – To Ground Fault Condition

During phase to ground fault for different operating conditions on secondary side, the MLE values of D coefficients of each phase are calculated as below:

R phase = 9.2616 (faulty phase)
S phase = 1.0119
T phase = 1.6242

R phase = 1.3277
S phase = 13.2414 (faulty phase)
T Phase = 1.0517

R phase = 1.5323
S phase = 0.4599
T phase = 29.0515 (faulty phase)

C. Two Phase – To Ground Fault Condition

During two - phase to ground fault for different operating conditions on secondary side, the MLE values of D coefficients of each phase are calculated as below:

R phase = **7.1622**
(faulty phases)
S phase = **23.3267**
T phase = 3.4420

R phase = 8.9181
S phase = **20.7463**
(faulty phases)
T phase = **35.9745**

R phase = 11.8410 ↘
S phase = 1.0201 **(faulty phases)**
T phase = 12.7242 ↗

As it is seen from the calculated MLE values of D coefficients, relay can easily conclude that there is a fault and sends a trip signal [12].

5. Conclusions

Very accurate and satisfactory results obtained with Coif6 wavelet transform yields the following conclusions:

- The wavelet decomposition breaks up the signals into both time and frequency, allowing for a more complete and efficient description of each phase current and accurate fault detection.
- Since this method is used for discontinuity analysis of the signals, even if the fault occurs at the lowest time space with a high impedance at the fault location, detail coefficients of the signal reveals the faulty condition.
- The required calculations are very simple, it is only necessary to perform a wavelet decomposition at level 2 for Coif6.
- The approach using Coif6 provides a marked important over FFT and Daubechies 4.

For a more novel approach, artificial neural network can be used for classification of faults in addition to detection scheme.

Acknowledgment

This research has been supported by Ondokuz Mayis University under the contract No: MF-047. The authors would like to acknowledge this support with gratitude.

Suggestions

This work is based on recorded data, which has been obtained from ATP-EMTP. For a future work, a real time digital signal processor can be used for analyzing current and voltage samples.

References

[1] M.A. Rahman, B. Jeyasurya", A State-of-The-Art Review of Transformer Protection Algorithms, IEEE Transactions on Power Delivery, Vol. 3, No. 2, April 1988.

[2] M.A. Rahman, B. So, M. R. Zaman, M.A. Hoque", Testing of Algorithms for A Stand-Alone Digital Relay for Power Transformers, IEEE Transactions on Power Delivery, Vol. 13, No. 2, April 1998.

[3] M. Habib, M.A. Marin", A Comparative Analysis of Digital Relaying Algorithms for Differential Protection of Three Phase Transformers, IEEE Transactions on Power Systems, Vol. 3. No. 3, August 1988.

[4] M. Fancisco, A.A. Jose, Wavelet Based ANN Approach For Transmission Line Protection, IEEE Power Engineering Review, 2003.

[5] G.-M. Moises, W.N. Denise, A Wavelet-Based Differential Transformer Protection, IEEE Transactions on Power Delivery, Vol. 14, No. 4, October 1999.

[6] O. Ozgonenel, G. Onbilgin, C. Kocaman, Wavelets and Its Applications of Power System Protection, Gazi University Technical Education Faculty, Journal of Politechnic, 17:2, P:75-88, 2004, ISSN: 1003:9709.

[7] M. Fedi, et al., Joint Application of Continuous and Discrete Wavelet Transform on Gravity Data to Identify Shallow and Deep Sources, International Journal of Geophys, 156, 7-21, 2004.

[8] Y.W. Seng, Q. Wang, A. Wavelet Based Method to Discriminate Between Inrush Current and Internal Fault, Power System Technology, 2000. Proceedings. PowerCon 2000. International Conference on, Volume: 2, 4-7 Dec. 2000, Page(s): 927 -931 vol. 2.

[9] L. M. Peilin, R.K. Aggarwal, A Novel, Approach to the Classification of the Transient Phenomena in Power Transformers Using Combined Wavelet Transform and Neural Network, IEEE Transactions on Power Delivery, Vol. 16, No. 4, October, 2002.

[10] M. Vannucci, P.J. Brown, T. Fearn, A Decision Theoretical Approach to Wavelet Regression on Curves With a High Number of Regressors. Journal of Statistical Planning and Inference, 112(1-2), 195-212, 2003.

[11] M. Vannucci, F. Corradi, Model Shrinking of Wavelet Coefficients and Applications. Proceedings of the Section on Bayesian Statistical Science, 1996 Joint Statistical Meetings, American Statistical Association. August 4-8, Chicago, Illinois, USA, pp. 117-123, 1996.

[12] Ç. Kocaman, Wavelet Based Transformer Protection Algorithm, Ondokuz Mayis University, Institute of Basic and Applied Sciences, MSc Thesis, 2003.